

Electronic Supplementary Information

Standing wave spectrometer with semi-transparent organic detector

Vladislav Jovanov,¹ Patrice Donfack,¹ Arne Müller,¹ Arnulf Materny,¹ Dietmar Knipp,² and Veit Wagner^{1,*}

¹ Department of Physics and Earth Sciences, Jacobs University Bremen, 28759 Bremen, Germany

² Geballe Laboratory for Advanced Materials, Department of Materials Science and Engineering, Stanford University, Stanford, CA 94305, USA

* E-mail: v.wagner@jacobs-university.de

Refractive index data for silicon and organic materials

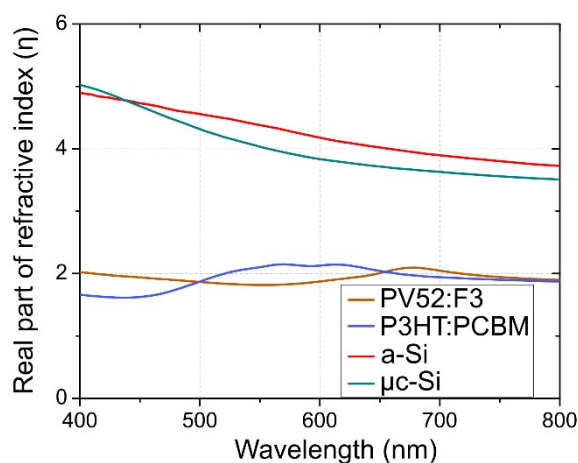


Figure S1. Real part of the refractive index for PV52:F3, P3HT:PCBM, a-Si and $\mu\text{c-Si}$ material. The data for a-Si and $\mu\text{c-Si}$ are adapted from literature.¹ The data for PV52:F3 and P3HT:PCBM are determined by fitting the reflectance and transmittance of single films on glass substrates measured by UV-VIS spectrometer.

¹ K. Ding, T. Kirchartz, B. E. Pieters, C. Ulbrich, A. M. Ermes, S. Schicho, A. Lambertz, R. Carius, and U. Rau, Characterization and Simulation of a-Si:H/ $\mu\text{c-Si:H}$ Tandem Solar Cells, Sol. Energy Mater. Sol. Cells 2011, 95, 12, 3318–3327.

AFM data

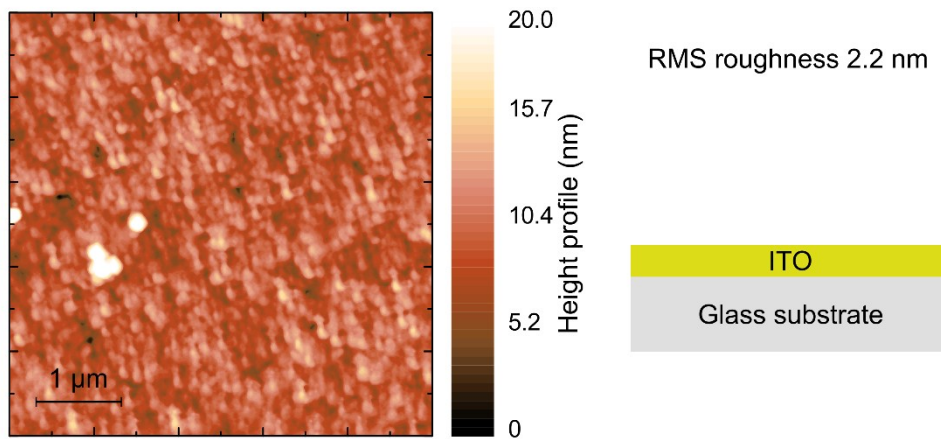


Figure S2. Topography of the ITO layer on top of the glass substrate. A root mean square roughness of 2.2 nm is determined for a scan area of $5 \times 5 \mu\text{m}^2$.

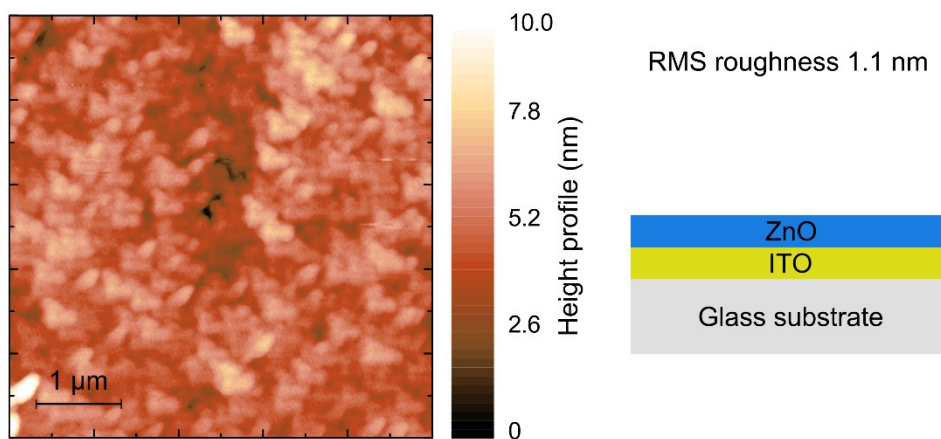


Figure S3. Topography of the ZnO layer deposited by spin-coating on top of the glass/ITO substrate. A root mean square roughness of 1.1 nm is determined for a scan area of $5 \times 5 \mu\text{m}^2$.

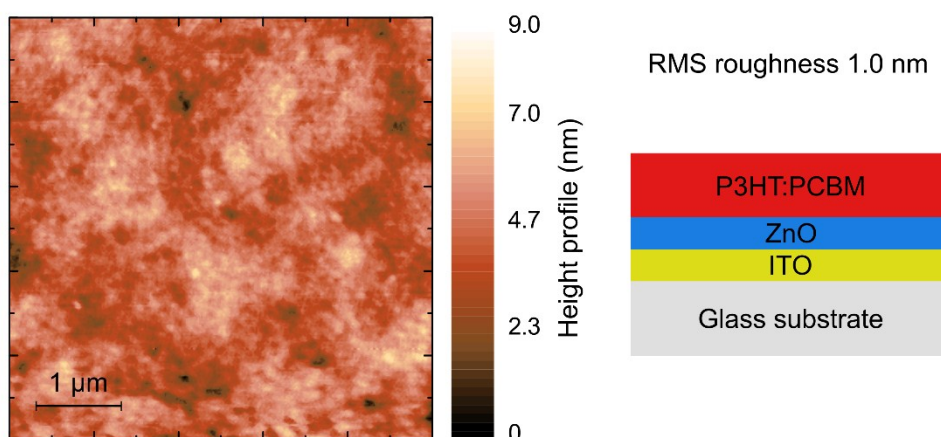


Figure S4. Topography of the P3HT:PCBM layer deposited by blading on top of the glass/ITO/ZnO substrate. A root mean square roughness of 1.0 nm is determined for a scan area of $5 \times 5 \mu\text{m}^2$.

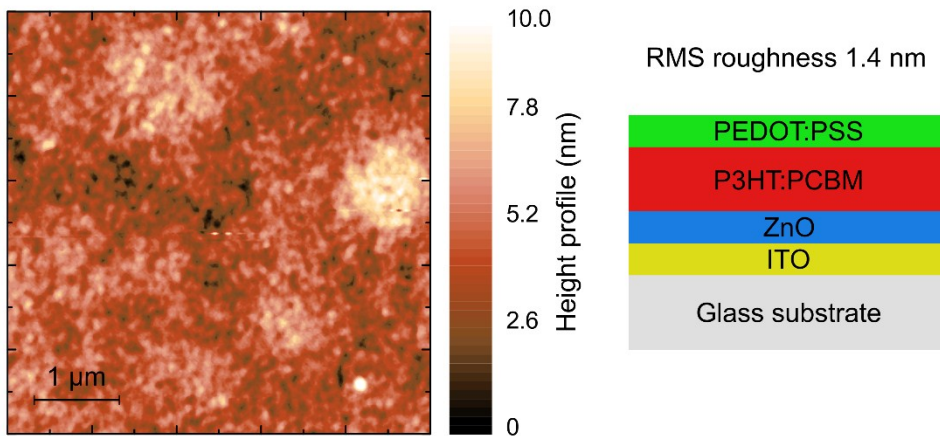


Figure S5. Topography of the PEDOT:PSS layer deposited by spin-coating on top of the glass/ITO/ZnO/P3HT:PCBM substrate. A root mean square roughness of 1.4 nm is determined for a scan area of $5 \times 5 \mu\text{m}^2$.

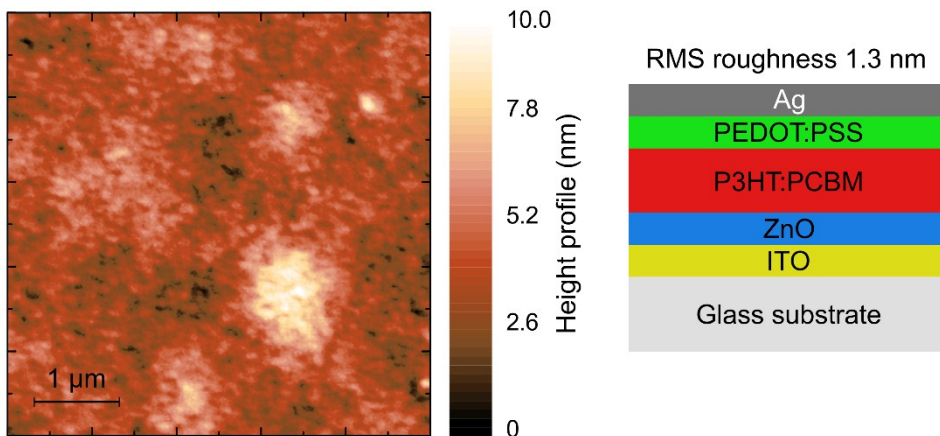


Figure S6. Topography of the silver layer deposited by sputtering on top of the glass/ITO/ZnO/P3HT:PCBM/PEDOT:PSS substrate. A root mean square roughness of 1.3 nm is determined for a scan area of $5 \times 5 \mu\text{m}^2$.

Optical and electrical characterization of P3HT:PCBM semi-transparent detector

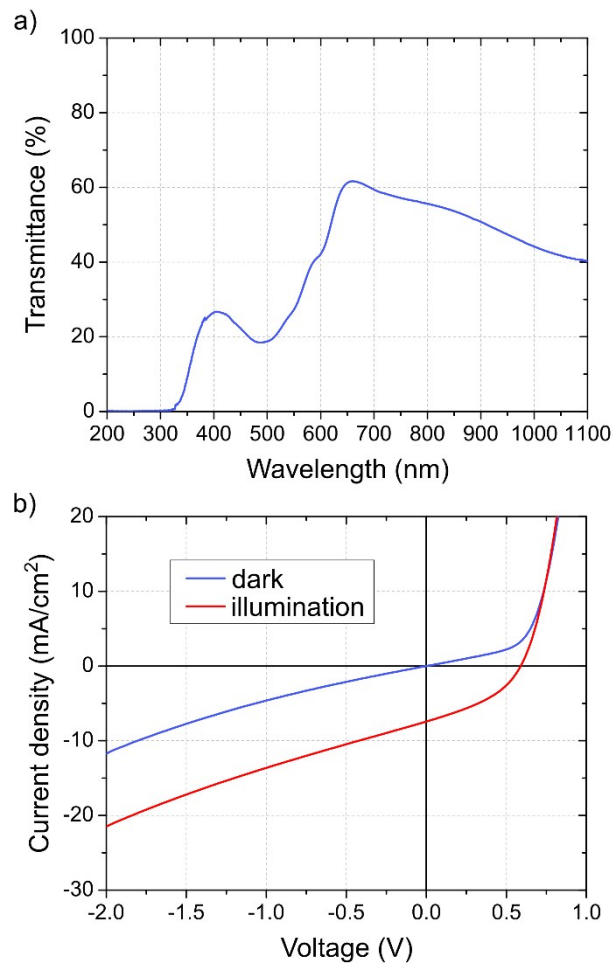


Figure S7. a) Transmittance and b) current-voltage curves (in dark and under AM 1.5 illumination) of a semi-transparent organic photo-detector based on a P3HT:PCBM blend.

Setup calibration – interferometry measurements with PV52:F3 semi-transparent detector

To determine the non-linearity of the piezo micro-actuator and exact mirror displacement during standing wave recording measurements, the standing wave setup is calibrated. The piezo-actuator is driven by the function generator with the same settings used for the realization of the spectrometer (see Manuscript). For this calibration, the Ar-ion laser line at 514.5 nm is used as test input. The semitransparent organic detector is used to record the interferogram. From the recorded interferogram, the standing wave nodes (zero values) and anti-nodes (minimum and maximum values) are extracted. The distance between these

characteristic points is $\lambda/8$, which allows us to determine the mirror displacement as a function of time. The corresponding results are shown in Figure S3.

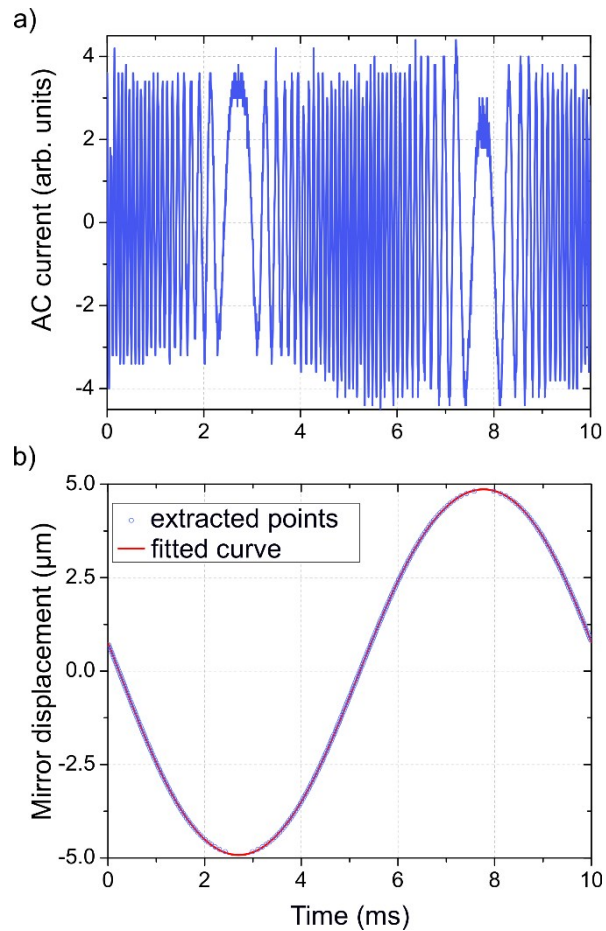


Figure S8. a) Recorded interferogram, b) extracted (anti-)node points (open circles), and fitted mirror displacement (full line) for the PV52:F3 detector obtained for an input wavelength of 514.5 nm.

Figure S3a depicts the recorded interferogram as a function of time. The mirror turning points are directly visible in Figure S8a from the slowing down of the current modulation at approx. 2.8 and 7.8 ms. The measured mirror displacement is shown in Figure S8b with open symbols. The extracted (anti-)node points are too far apart to accurately map the mirror displacement close to the turning points of the mirror. Therefore, the extracted points are fitted by a cosine function with first, second, and third order harmonics given by:

$$f_{fit}(t) = \sum_{j=1}^3 A_j \cdot \cos(2 \cdot \pi \cdot j \cdot f_0 \cdot t + \phi_j) \quad (S1)$$

where f_0 is the fundamental frequency, A_j is the amplitude and ϕ_j is the phase shift of the respective harmonic. The determined parameters for the fit function are given in Table S1.

Table S1. Parameters for the fit function determined from the mirror displacement curve (Figure S8b).

Parameters	Harmonics		
	First order j=1	Second order j=2	Third order j=3
Frequency – f_0 (Hz)	99.95		
Amplitude – A_j (μm)	4.983	0.052	0.092
Phase – ϕ_j ($^\circ$)	82.02	38.51	72.22

The parameters presented in Table S1 show that for the realized setup the contribution of higher order harmonics is about 1 - 2% of the fundamental and should be included for proper data analysis. The resulting recording length (L_R) of the standing wave pattern, which is the maximum traveling distance of the mirror, is calculated to be 9.784 μm .

Gaussian envelope.

Envelope function:

$$f_{envp}(\Delta z_m) = \exp\left(-\frac{16 \cdot \Delta z_m^2}{L_R^2}\right) \quad (S2)$$

with Δz_m being the mirror displacement and L_R the recording length. The value of the recording length is determined from the setup calibration.

Theoretical value for FWHM for the spectral feature around central wavelength (λ):

$$FWHM_{Gauss} = \frac{4 \cdot \lambda^2}{\pi \cdot L_R} \ln(\sqrt{2}) \quad (S3)$$

P3HT:PCBM semi-transparent detector – setup calibration and spectrometry

measurements

The result of a setup calibration with the P3HT:PCBM semi-transparent detector is shown in Figure S9. For setup calibration and spectroscopy measurements, the piezo actuator is driven by a cosine voltage with a frequency of 45 Hz provided by a function generator. The Kr-ion laser line at 647.1 nm is used as test input during setup calibration. As fitting function we have again used Equation (S1) and the fit parameters are given in Table S2.

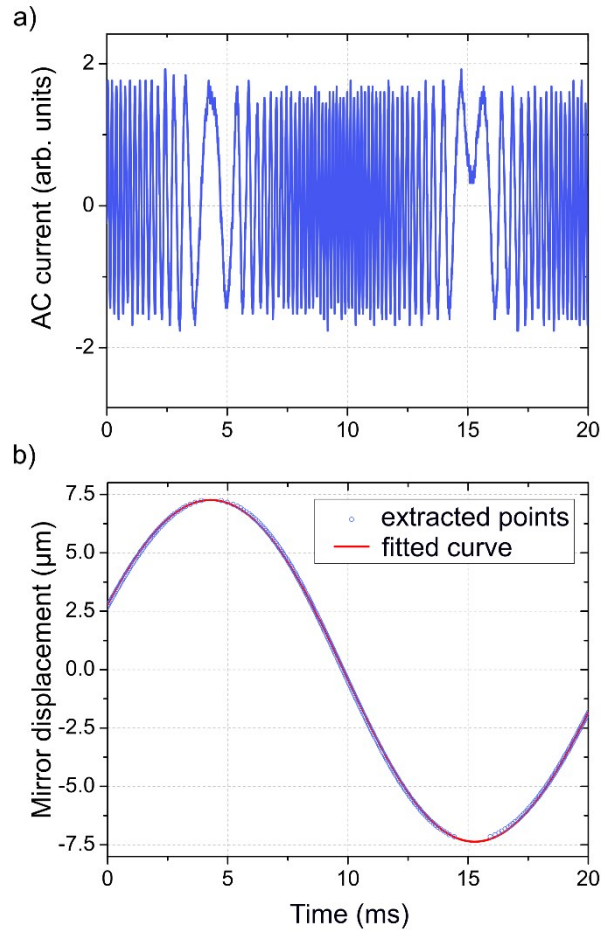


Figure S9. a) Recorded interferogram, b) extracted (anti-)node points (open circles), and fitted mirror displacement (full line) for the P3HT:PCBM detector obtained for an input wavelength of 647.1 nm.

Table S2. Parameters for the fit function determined from the mirror displacement curve (Figure S9b).

Parameters	Harmonics		
	First order $j=1$	Second order $j=2$	Third order $j=3$
Frequency – f_0 (Hz)	44.998		
Amplitude – A_j (μm)	7.395	0.079	0.081
Phase - ϕ_j ($^\circ$)	52.94	-26.00	-23.76

The resulting recording length (L_R) is calculated to be 14.63 μm .

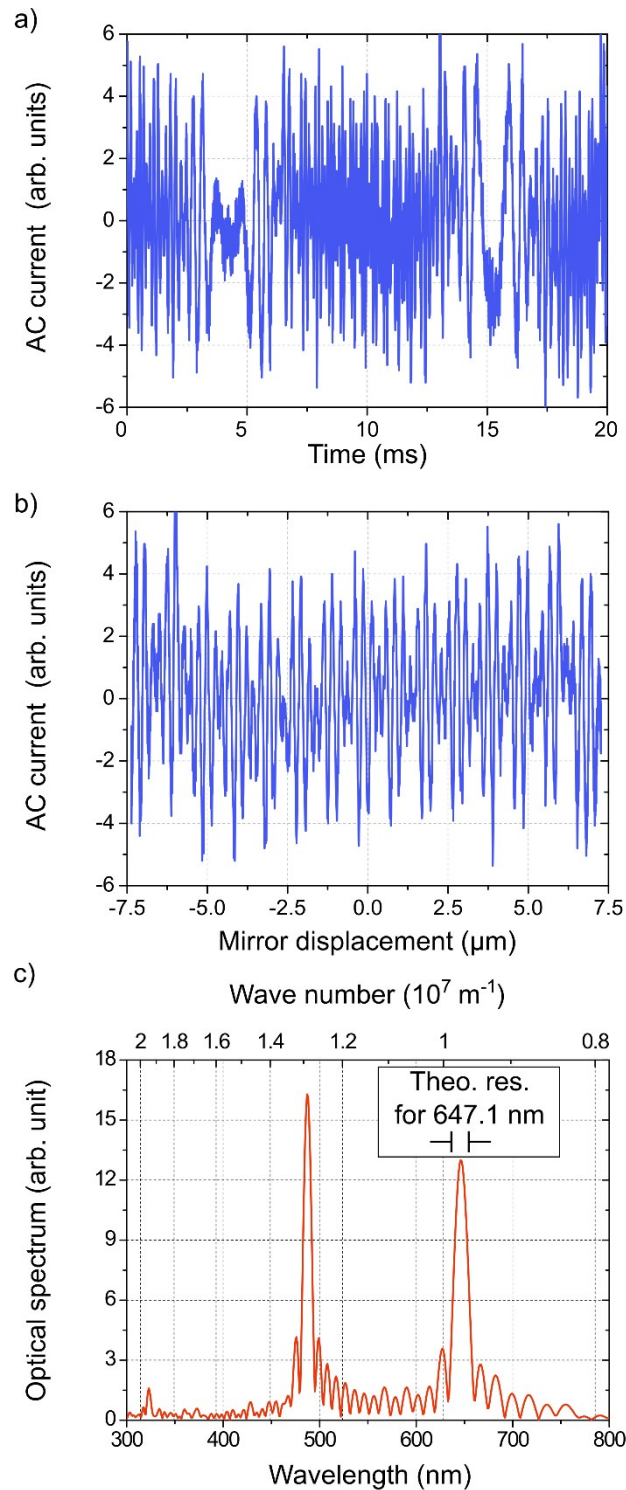


Figure S10. The AC current recorded by the P3HT:PCBM semi-transparent detector as a function of a) time and b) mirror displacement (Δz_m) under combined illumination from the Ar- (488 nm) and Kr-ion lasers (647.1 nm). c) Spectrum of the test input determined by Fourier transform and without applying the Gaussian envelope.

For the spectrometer measurements, a combined illumination by the Ar-ion laser (514.5 nm) and the Kr-ion laser (647.1 nm) is used as test input. The current generated by the P3HT:PCBM semi-transparent organic detector is recorded as a function of time (Figure S10a) and then remapped as a function of mirror displacement (Figure S10b). The corresponding spectrum is given in Figure S10c. To suppress unwanted side peaks, the Gaussian envelope (Equation (S3)) is used (see Figure S11).

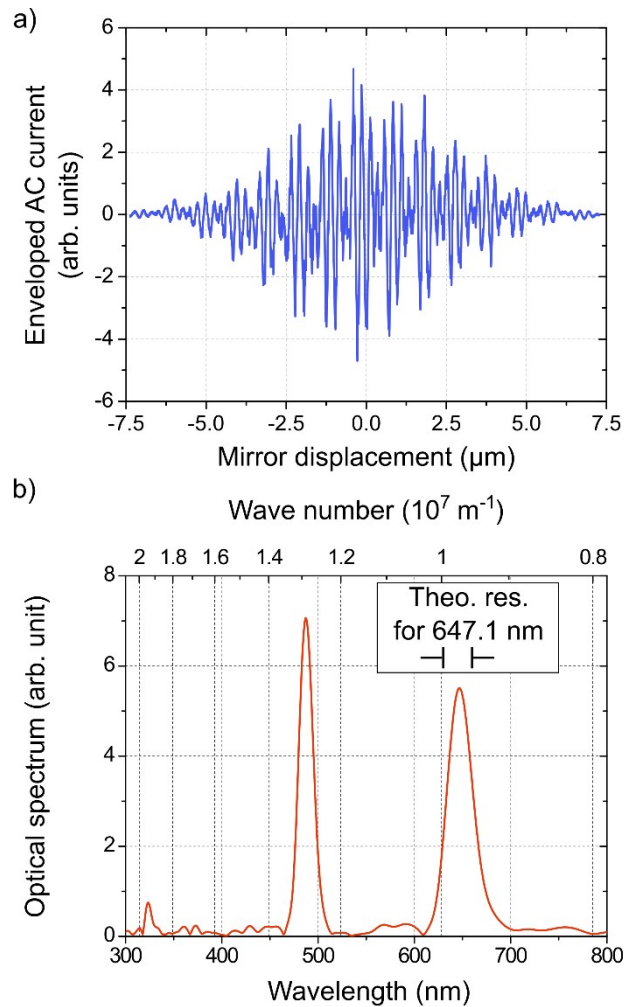


Figure S11. a) Spectrogram enveloped by a Gaussian function measured by the P3HT:PCBM semi-transparent detector. b) Spectrum of the test input (combined illumination from an Ar-ion laser (488 nm) and a Kr-ion (647.1 nm) laser) determined by Fourier transform.

The intensity of the peak at 647.1 nm is larger compared to that obtained with the PV52:F3 semi-transparent detector since the transmittance of P3HT:PCBM is higher in this wavelength region.

Analytical model of the standing wave spectrometer

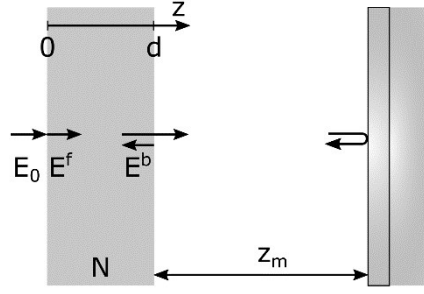


Figure S12. Simple model of the semi-transparent photodetector as standing wave sensing device.

Figure S4 schematically depicts a simplified model of the standing wave sensing device. The semi-transparent detector is described only by its thickness d and its complex refractive index $N = \eta - i\kappa$, where η is the real part or refractive index and κ the imaginary part or extinction coefficient. Assuming that there is no reflection at the interfaces of semi-transparent detector, the electric field within the detector can be expressed as a sum of forward and backward propagating waves:

$$E(z) = E^f \cdot e^{-i \cdot k_N \cdot z} + E^b \cdot e^{i \cdot k_N \cdot (z-d)} \quad (\text{S4})$$

where E^f and E^b are the electric field amplitudes of the forward and backward propagating wave, respectively, and $k_N = 2\pi \cdot N/\lambda$ is the wave number within the detector with λ being the vacuum wavelength of the incoming light. Under given assumptions, the relationship between electric field amplitudes of forward and backward waves can be written as:

$$E^b = E^f \cdot e^{-i \cdot (k_N \cdot d + 2 \cdot k \cdot z_m + \pi)} \quad (\text{S5})$$

where $k = 2\pi/\lambda$ is the vacuum wave number of the light, z_m is the distance between detector and the mirror (see Figure S4), and the addition of π represents the phase shift introduced by

the mirror assuming that it reflects light perfectly. Finally, the total electric field within the detector can be rewritten to:

$$E(z) = E^f \cdot [e^{-i \cdot k_N \cdot z} + e^{-i \cdot (k_N \cdot (2 \cdot d - z) + 2 \cdot k \cdot z_m + \pi)}] \quad (\text{S6})$$

The absorbed power can be calculated as:

$$P_{loss} = \frac{1}{2} \cdot \int_V j^* \cdot E \cdot dV = \frac{1}{2} \cdot \int_V \sigma \cdot E^* \cdot E \cdot dV = \frac{1}{2} \cdot \int_V \sigma \cdot |E|^2 \cdot dV \quad (\text{S7})$$

where the conductivity (σ) can be connected to the complex refractive index based on the wave equation:

$$\sigma = \epsilon_0 \cdot c \cdot \eta \cdot \frac{4 \cdot \pi \cdot \kappa}{\lambda} = \epsilon_0 \cdot c \cdot \eta \cdot \alpha \quad (\text{S8})$$

where c is the speed of light, ϵ_0 is the dielectric permittivity of vacuum, and α is the absorption coefficient. Since we analyze a 1D model, the absorbed power can be expressed as:

$$P_{loss} = \frac{1}{2} \cdot \epsilon_0 \cdot c \cdot \eta \cdot \alpha \cdot A \cdot \int_0^d |E(z)|^2 \cdot dz \quad (\text{S9})$$

where A is the active area of the detector. Under the assumption that all charge carriers generated by light are extracted, the photo-generated current can be expressed as:

$$I_{ph} = \frac{q}{h \cdot \nu} \cdot P_{loss} \quad (S10)$$

where q is the elementary charge, h is Planck's constant and $\nu = c/\lambda$ is the frequency of light.

By replacing the conductivity σ in Equation (S7) using the expression given in Equation (S8) and solving the integral we get:

$$I_{ph} = \frac{1}{2} \cdot \frac{q}{h} \cdot \epsilon_0 \cdot \lambda \cdot A \cdot \eta \cdot |E^f|^2 \cdot \left[(1 - e^{-2 \cdot \alpha \cdot d}) - \frac{\lambda}{\eta \cdot \pi} \cdot \alpha \cdot e^{-\alpha \cdot d} \cdot \sin\left(\frac{2 \cdot \pi}{\lambda} \cdot \eta \cdot d\right) \cdot \cos\left(\frac{2 \cdot \pi}{\lambda} \cdot \eta \cdot d\right) \right] \quad (S11)$$

Since there is no reflection at the interface of the semi-transparent detector, the light intensity just inside of the detector (I_N) should be equal to the input light intensity (I_0), which leads to:

$$I_0 = I_N \Rightarrow |E_0|^2 = \eta \cdot |E^f|^2 \quad (S12)$$

and the photocurrent is finally given by:

$$I_{ph} = I_{ph0} \cdot \left[(1 - e^{-2 \cdot \alpha \cdot d}) - \frac{\lambda}{\eta \cdot \pi} \cdot \alpha \cdot e^{-\alpha \cdot d} \cdot \sin\left(\frac{2 \cdot \pi}{\lambda} \cdot \eta \cdot d\right) \cdot \cos\left(\frac{2 \cdot \pi}{\lambda} \cdot \eta \cdot d + \frac{4 \cdot \pi}{\lambda} \cdot z_m\right) \right] \quad (S13)$$

where $I_{ph0} = \frac{1}{2} \cdot \frac{q}{h} \cdot \epsilon_0 \cdot \lambda \cdot A \cdot |E_0|^2$ represents the generated current if all the incoming light gets absorbed by the detector.